

# STOCHASTIC ANALYSES OF DYNAMIC FRACTURE IN COMPOSITE CERAMIC MICROSTRUCTURES

VIKAS TOMAR & MIN ZHOU

School of Mechanical Engineering, Georgia Institute of Technology, Atlanta, GA 30332-0405, U.S.A.

## ABSTRACT

Variations in constituent properties, phase morphology, and phase distribution cause deformation and failure at the microstructural level to be inherently stochastic. This paper focuses on the stochasticity of fracture processes that arises as a result of measurement uncertainties in the properties of the constituents in the heterogeneous microstructures of an  $\text{Al}_2\text{O}_3/\text{TiB}_2$  ceramic composite system. A micromechanical cohesive finite element framework with explicit resolution of arbitrary fracture patterns and arbitrary microstructural morphologies is used. A deterministic analysis and a stochastic analysis are carried out simultaneously. The combination of determinism and stochasticity is achieved by integrating a perturbation analysis of the influence of stochastic property variations around their mean values and a deterministic analysis for the microstructure with the mean values of the constituent properties. Calculations are carried out for actual and idealized microstructures of the  $\text{Al}_2\text{O}_3/\text{TiB}_2$  material system. It is found that for the system analyzed the variations in the crack surface area generated and the variations in the energy release rate are of the same order as the variations in constituent properties.

## 1. INTRODUCTION

The stochasticity in material behavior arises out of several factors. Arbitrary microstructural phase morphologies and material heterogeneities are one source. The variations of local properties from specimen to specimen are another source. The statistical quantification of fracture behavior of a material should be based on a proper consideration of the correlation among three elements: probability distributions characterizing the distribution of flaws and material properties, fracture mechanics and material microstructure. Commonly used approaches for statistical characterization of fracture in brittle materials based on the Weibull theory<sup>1</sup> are almost exclusively based on the first element. Progress has been made in incorporating the other two elements into the Weibull theory<sup>2</sup>. However, until recently there was no general approach for the analysis of fracture with explicit account of microstructural morphology, random variation of material properties, and fracture processes. Recently, one such finite element framework has been developed<sup>3</sup>. With this framework, it is possible to obtain from one single calculation both a deterministic quantification of a fracture process and an estimate of the range of possible fracture outcome in terms of quantities such as stress distribution, strain field, crack length, crack speed, and energy release rate. This method is used here to characterize the effect of the random variations in material properties on the dynamic fracture behavior of an  $\text{Al}_2\text{O}_3/\text{TiB}_2$  ceramic composite system.

## 2. COMPUTATIONAL SETUP

Our approach for combined deterministic and stochastic analyses with explicit account of microstructure and fracture processes integrates the micromechanical cohesive finite element method<sup>4</sup> (CFEM) and a second order perturbation analysis for linear finite element problems<sup>5</sup>. This integration involves the superposition of the perturbation analysis on top of the CFEM deterministic analysis of fracture<sup>3</sup>. Specifically, the deterministic analysis is carried out for the material whose properties at each point are equal to the expectation values of the corresponding

material parameters. The perturbation analysis is relative to the deterministic state at each time, with respect to the variations in material parameters. While the deterministic process follows the standard field equations of balance of momentum, kinematic, and constitutive equations, the perturbation analysis yields a sequential system of differential equations for the successive derivatives up to the second order of the displacement. The successive derivatives of the displacement field are then used to characterize the stochastic outcome of material behavior. This characterization is in terms of the expectation value and the variance of quantities quantifying the deformation and failure of the microstructures analyzed (e.g., stress, crack length, and energy dissipated). While the deterministic analysis explicitly tracks fracture processes, the perturbation analysis focuses on the mean and standard deviations of independent variables (material properties) and dependent variables. The analysis is valid only for conditions under which variations in independent variables have narrow band characteristics and fluctuations of small magnitudes. Therefore, perturbation analyses up to the second order can be carried out<sup>6</sup> and only variations of up to 15% relative to mean values can be considered.

Computations are carried out for a center-cracked  $\text{Al}_2\text{O}_3/\text{TiB}_2$  specimen under tensile loading. The finite element mesh used consists of “cross-triangle” elements of equal dimensions arranged in a quadrilateral pattern. Cohesive surfaces are embedded along all finite element boundaries as part of the physical model. The whole specimen has a width of  $2W=2\text{ mm}$  and a height of  $2H=0.6\text{ mm}$ . The length of the initial crack is  $2a_i=0.4\text{ mm}$ , see Fig. 1. The specimen is stress free and at rest initially. Tensile loading is applied by imposing symmetric velocity boundary conditions along the upper and the lower edges of the specimen. For the results discussed here, the imposed boundary velocity of  $V_0=2\text{ m/s}$  is applied on the top and bottom edges with a linear ramp from zero to this maximum velocity in the first  $0.01\text{ }\mu\text{s}$  of loading. Conditions of plain strain are assumed to prevail. The size of the quadrilaterals in the mesh is  $2\text{ }\mu\text{m}$ . The calculations of this paper involve nine nodal points and bilinear shape functions for property interpolation, see Fig. 1.

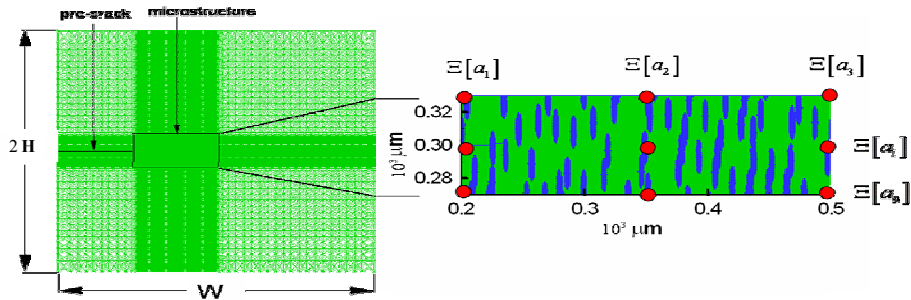


Figure 1: A schematic illustration of the stochastic model

The model parameters are the same those in Ref. 4. During the analysis, the expected value of a material property is taken to be the same as its deterministic value and the stochastic variation is relative to the expected values. Also in this paper, the expected values of materials constants for each phase in a microstructure are spatially homogenous. Under this condition here, the zeroth-order stochastic moment of any dependent quantity (e.g., displacement, a stress component, a strain component, dissipated energy, a cohesive surface traction component, or a component of the cohesive surface separation) corresponds to the deterministic value, allowing integrated deterministic and stochastic analyses to be carried out. The cumulative probability of the range of outcome is calculated using Chebyshev inequality<sup>7</sup> and corresponds to a minimum of 99.973%.

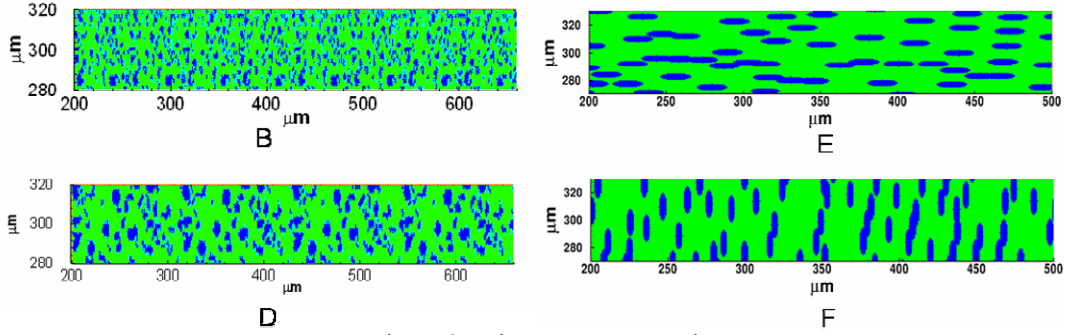


Figure 2: Microstructures used.

Figure 2 shows the microstructures used in the analyses. The labeling of these microstructures follows the convention in Ref. 4 for the ease of direct comparison with the deterministic results. The volume fraction of the  $\text{TiB}_2$  phase in all four microstructures is 30%. While consisting of the same type of particles, microstructures E and F have two different particle arrangements, representing two orthogonal microstructural orientations. Microstructures B and D are actual phase distributions of materials produced in the laboratory. These microstructures consist of  $\text{TiB}_2$  particles (with average linear intercept length values of approximately  $2 \mu\text{m}$  and  $3 \mu\text{m}$ , respectively) surrounded by an  $\text{Al}_2\text{O}_3$  phase (with average linear intercept length of approximately  $5 \mu\text{m}$  and  $8 \mu\text{m}$ , respectively). There is a clear difference in the size scales of the phases between the two microstructures.

### 3. RESULTS

Figure 3 shows the time histories of the expected value of total energy dissipated  $\Phi$ , which is defined as  $\Phi = \int_{S_0} \Phi_d dS$  ( $\Phi_d$  is energy dissipated per unit cohesive surface area), for all four microstructures.

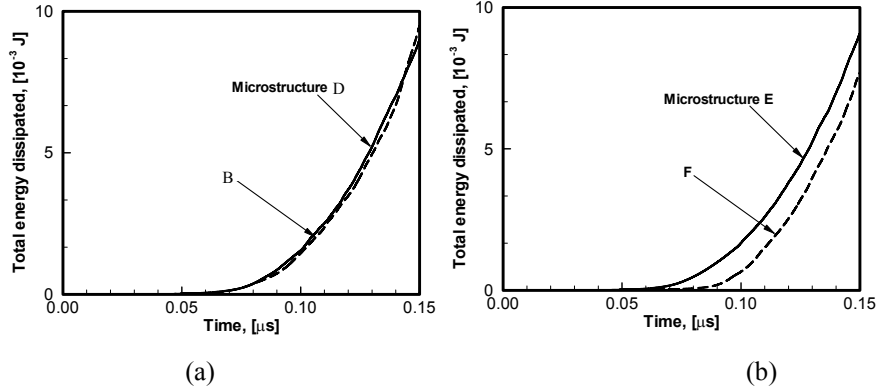


Figure 3: Time histories of the expected value of total energy dissipated for different microstructures

While the difference between the profiles for microstructures B and D is small, the difference between the profiles for microstructures E and F is significant. This indicates that, when all microstructures assume fixed deterministic values of material properties which are equal to their expected values, the difference between the fracture resistances of microstructures B and D is

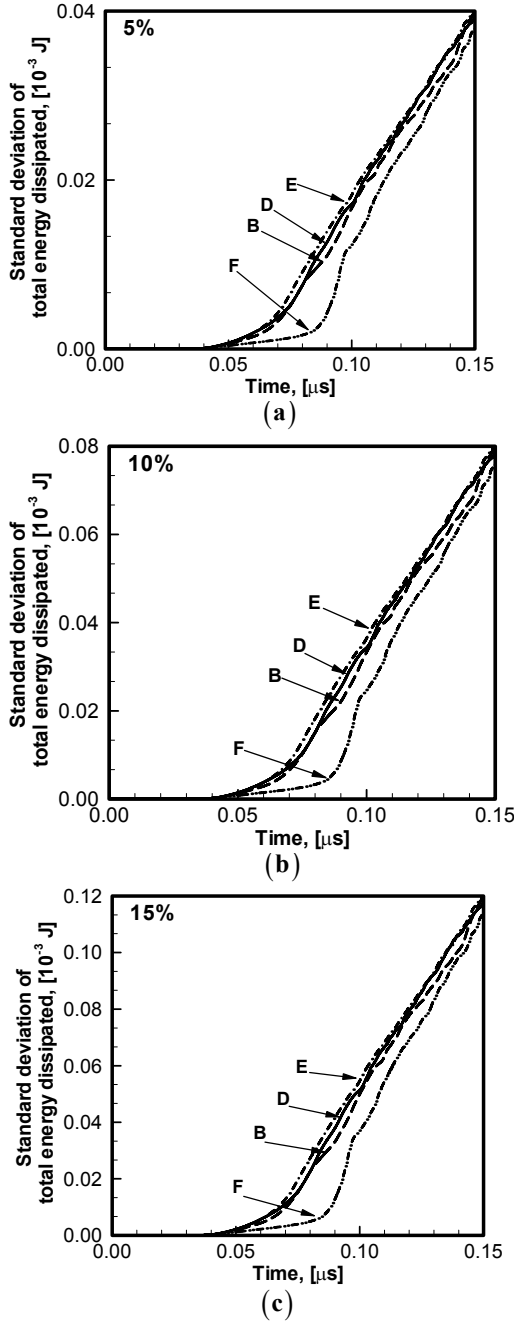


Figure 4: Time histories of the standard deviation of total energy dissipated for different microstructures at different levels of variations of interfacial properties, the variation of the bulk properties is held at 0%.

smaller compared with the difference between the fracture resistances of microstructures E and F. Also under such conditions, microstructure F shows the highest resistance to fracture initiation since it has a crack initiation times of approximately 0.09  $\mu\text{s}$  while microstructures B, D, and E have fracture initiation times of approximately 0.07  $\mu\text{s}$ . To compare the variations of fracture resistances of these microstructures, their time histories of standard deviation of total energy dissipated is plotted in Fig. 4. Three different levels of variation (5%, 10%, 15%) for the interfacial properties ( $T_{max}$  and  $\Delta_{nc}$ ) are considered while the variation of the bulk properties ( $E$  and  $\nu$ ) is held at 0%. The variation in the energy dissipated clearly depends on the microstructures and is highly sensitive to the variation in interfacial properties. In all four microstructures, the average coefficient of variation (the ratio of standard deviation and expected value which is a measure of the spread of a statistical distribution around the mean value) of the total energy dissipated is approximately 0.005, 0.01, and 0.015 when the variation of the interfacial properties is at 5%, 10%, and 15%, respectively. This trend is weakly dependent on the microstructural morphology involved. Specifically, the range of variation is larger for microstructure E than for microstructure F which has a lower level of expected value of energy dissipated than microstructure E at any give time as seen in Fig. 3. While the lower expected value of the energy dissipated in microstructure F signifies a higher resistance to crack propagation, the higher range of variation of the energy dissipated for microstructure E signifies the possibility of a wider range of variation in fracture outcome in terms of, e.g., crack path and crack length. Such a wider range of variation almost invariably leads to lower fracture resistance in a statistically sense since cracks follow the weakest path. A similar trend of wider range of variation with lower expected value

of the energy dissipated is seen for microstructures B and D as well. To quantify the range of behavior variation, the standard deviation of the total energy dissipated ( $s_d^\phi$ ) is used to evaluate an upper limit and a lower limit for the energy release rate.

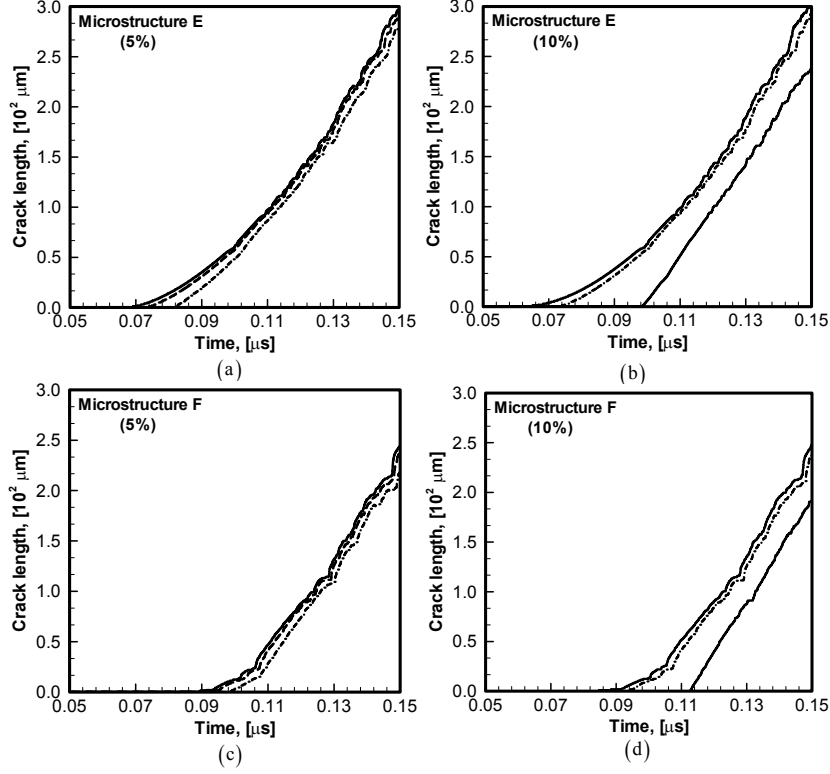


Figure 5: Time histories of the range of crack length in microstructures E and F at different levels of property variations (the three curves give the upper limit, the expected value and the lower limit of crack length, respectively)

Specifically, the range is  $\mu^\phi \pm 6s_d^\phi$ . Similarly, the coefficient of variation of the interfacial state variable  $\lambda$  ( $s_d^\lambda$ ) is used to obtain a range of variation for crack length which is taken as  $\mu^\lambda \pm 6s_d^\lambda$ . Figure 5 shows the time histories of the range of crack length for microstructures E and F at two different levels (5% and 10%) of variation of interfacial properties. Clearly, microstructure has a clear impact on the fracture initiation time. For microstructure E, the average deviation of crack length to the lower side is approximately 6% of the expected value for a 5% variation of interfacial properties and approximately 20% of the expected value for a 10% variation of interfacial properties. For microstructure F, the average deviation to the lower side is approximately 8% of the expected value for a 5% variation of the interfacial properties and approximately 25% of the expected value for a 10% variation of the interfacial properties. The deviation to the upper side is much less, at approximately 2% to 5% of the expected value for variations of interfacial properties between 5% and 10% for microstructure E. For microstructure F, the deviation to the upper side is approximately 3% to 6% of the expected value for the same amount of variation in properties. The expected value of the total crack length and its variation for microstructures B and D follow a similar trend as seen in Fig. 5 for microstructures E and F.

The range of energy release rate was calculated for the four microstructures at time  $t=0.15 \mu\text{s}$  for levels of variation upto 15% (The range of this average energy release rate is characterized by  $\bar{G}_{low} = \phi_d^{low} / l^{low}$ ,  $\bar{G}_{exp} = \phi_d^{expect} / l^{expect}$ , and  $\bar{G}_{high} = \phi_d^{upper} / l^{upper}$ , with  $l^{low}$ ,  $l^{exp}$ , and  $l^{high}$  denoting the lower

limit, mean, and upper limit of crack length  $l$ , respectively). Significant variations are observed for all microstructures with the increase in the level of variation of interfacial properties. Specifically for microstructures E and F, approximately 3% to 6% variations relative to their expected values are seen for variations of interfacial properties between 5% and 10%. For microstructures B and D, approximately 2.5% to 4% variations relative to their expected values are seen for variations of interfacial properties between 5% and 10%. The range of energy release rate is wider for microstructure F than for microstructure E. Similarly, the range of energy release rate is wider for microstructure D than for microstructure B. The larger particle size in microstructure D relative to that in microstructure B appears to give rise to the higher level of variation in the energy release rate. For all microstructures, the difference between the upper limit and the expected value of the average energy release rate is higher than the difference between the expected value and the lower limit of the average energy release rate. This again indicates that an increase in the random variation of properties has an asymmetric effect on the variation of the energy release rate. Note that the analysis here concerns only the range of variation and does not address the issue of probability distribution of events. This result only suggests that, with random variations of properties, the difference between the maximum and the expected values of the energy release rate is larger than the difference between the expected and the minimum values.

#### 4. CONCLUSION

A framework for combined deterministic and stochastic analyses of dynamic fracture in heterogeneous microstructures is used to analyze dynamic fracture in idealized and real microstructures of a two-phase  $\text{Al}_2\text{O}_3/\text{TiB}_2$  ceramic composite system. The effect of random variations in material properties of up to 15% from their mean values is analyzed with an explicit account of random crack development. Calculations show that the lower bound for the fracture response is very close to the response of a material whose phases possess the expectation values of the randomly varying material properties. In addition, the effect of property variations on the variation of crack length, energy dissipation, and damage is not symmetric, reflecting the fact that cracks tend to follow the weakest path.

#### ACKNOWLEDGMENTS

This work is supported by US ARO through DAAG55-98-1-0454 and US NSF through CMS9984298. Calculations are carried out at the NAVO and ERDC MSRCs.

#### REFERENCES

1. Weibull, W. "A statistical distribution function of wide applicability", *ASME J. Appl. Mech.*, Vol. 18, No. 3, 1951, pp. 293-297.
2. Dai, H. and Frantziskonis, G., "Heterogeneity, spatial correlations, size effects and dissipated energy in brittle materials", *Mech. Mat.*, Vol. 18, No. 1994, pp. 103-118.
3. Tomar, V. and Zhou, M., "Deterministic and stochastic analyses of dynamic fracture in two-phase ceramic microstructures with random material properties", *manuscript in preparation*, Vol. No. 2004.
4. Zhai, J., Tomar, V. and Zhou, M., "Micromechanical modeling of dynamic fracture using the cohesive finite element method", *J. Engg. Mat. Tech.*, Vol. 126, No. 2004, pp. 179-191.
5. Liu, W. K., Belytschko, T. and Mani, A., "Random field finite elements", *Int. J. Num. Meth. Engg.*, Vol. 23, No. 1986, pp. 1831-1845.
6. Ghanem, R. G. and Spanos, P. D., "Stochastic finite elements: A spectral approach", Springer-Verlag, New York, 1991.
7. Nigam, N. C. "Introduction to random vibrations", The MIT press, Cambridge, MA, 1983.